

# Arbitrary-ratio $1 \times 2$ power splitter based on asymmetric multimode interference

Qingzhong Deng, Lu Liu, Xinbai Li, and Zhiping Zhou\*

State Key Laboratory of Advanced Optical Communication Systems and Networks, School of Electronics Engineering and Computer Science, Peking University, Beijing 100871, China

\*Corresponding author: zjzhou@pku.edu.cn

Received July 30, 2014; accepted August 21, 2014;  
posted August 27, 2014 (Doc. ID 220028); published September 22, 2014

Free choice of splitting ratio is one of the main properties of a power splitter required in integrated photonics, but conventional multimode interference (MMI) power splitters can only obtain a few discrete ratios. This Letter presents both numerical and experimental results of an arbitrary-ratio  $1 \times 2$  MMI power splitter, which is constructed by simply breaking the symmetry of the multimode region. In the new device, the power splitting ratio can be adjusted continuously from 100:0 to 50:50, while the dimension of the multimode section stays in the range of  $1.5 \times (1.8\text{--}2.8)$   $\mu\text{m}$ . The experimental data also indicate that the proposed arbitrary-ratio splitter keeps the original advantages of MMI devices, such as low excess loss, weak wavelength dependence, and large fabrication tolerance. © 2014 Optical Society of America

OCIS codes: (130.3120) Integrated optics devices; (130.1750) Components; (230.1360) Beam splitters.

<http://dx.doi.org/10.1364/OL.39.005590>

Recently, integrated photonics has attracted considerable attention for its complementary functions and compatible fabrication process with integrated electronics [1]. A power splitter is an essential component for integrated functional photonics systems. A multimode interference (MMI) power splitter plays an important role in the development of integrated photonics due to large fabrication tolerance, wide operation bandwidth, and compact size [2]. Free choice of power splitting ratio is one of the important properties for the applications of photonic integrated circuits (PICs), such as a nanophotonic phased array [3], an optical power tap [4], an asymmetric Mach-Zehnder interferometer (MZI) [5,6], and ladder-type optical filters [7]. However, the conventional MMI power splitter with two output ports can only obtain splitting ratios of 100:0, 85:15, 72:28, and 50:50 through adjusting the position of input and output ports [8,9]. Several methods have been reported aiming at an arbitrary-ratio MMI power splitter, such as butterfly-like MMI splitters [10], bent MMI splitters [11,12], MMI with computer-generated planar holograms [13,14], cascaded MMI couplers with unequal width [15–17], MMI splitter with cladding-filled gap [18], and multiple-arm MZI consisting of an active phase-shifting region placed between two MMI couplers [19]. However, all these methods suffer from relatively complex structures and large footprints. In this Letter, we propose and experimentally demonstrate a compact arbitrary-ratio  $1 \times 2$  power splitter based on a simple asymmetric MMI structure.

The schematic of the conventional symmetric  $1 \times 2$  MMI power splitter is shown in Fig. 1(a). TE-polarized light is, through the single-mode input waveguide ( $WG_{in}$ ), transmitted to the multimode region, where MMI is excited. Then, the light is tapered into two single-mode output waveguides ( $WG_{up}$  and  $WG_{bot}$ ) symmetrically at the first two-fold image distance. Due to the structural symmetry, the splitter only allows uniform split of the incident light into two output waveguides, as indicated in the energy flux density [Figs. 1(c) and 1(d)] and optical field [Figs. 1(g) and 1(h)]. On the other hand, there is little energy and field distribution in the left

corners of the multimode region [marked with dashed red ellipses in Figs. 1(c) and 1(g)]. Even though these corners contain little optical field, removing one of them will break the symmetry of interference, in accordance with the self-imaging principle [20]. Such asymmetric MMI, excited by asymmetric perturbation in the multimode region, will have a significantly different optical field distribution.

The proposed asymmetric MMI power splitter is shown in Fig. 1(b). Compared to the conventional symmetric power splitter, the only difference is that the symmetry of the multimode region is broken by removing its bottom left corner (marked with a red dashed rectangle). Such a minor structural change causes a dramatic redistribution of the optical field [Figs. 1(e), 1(f), 1(i), and 1(j)]. If the output waveguides are also located at the position of the first two-fold image, the power output from  $WG_{up}$  will be greater than that from  $WG_{bot}$  as shown in Figs. 1(f) and 1(j). Furthermore, the unevenness of this power splitting will increase as the removed rectangle becomes longer [the width keeps constant, Fig. 1(k)]. Based on these phenomena, the arbitrary-ratio power splitter can be obtained by adjusting the dimension of the removed region.

Prototype devices were fabricated on silicon-on-insulator (SOI) wafers, with 220 nm top silicon and 2  $\mu\text{m}$  thick buried oxide by electron-beam lithography, followed by inductively coupled plasma etching. The top view of the device is shown in the scanning electron microscope (SEM) image [Fig. 2(a)]; a rectangle of 400 nm in width ( $W_r$ ) and variable lengths ( $L_r$ ) were removed from the bottom left corner of the fabricated asymmetric MMI splitters. The various lengths ( $L_r$ ) were designed for different power splitting ratios [ $L_r = 0.4$   $\mu\text{m}$  in Fig. 2(a)]. To characterize these splitters, a tunable CW laser of TE-polarization is butt-coupled into the chip through a tapered lens fiber. The optical images [Figs. 2(b)–2(f)], captured from the output waveguides, confirm the phenomenon observed by simulations that more optical power is output from  $WG_{up}$ , while the removed rectangle from the bottom left corner becomes longer. To analyze these power splitting ratios (PSRs, defined as the output

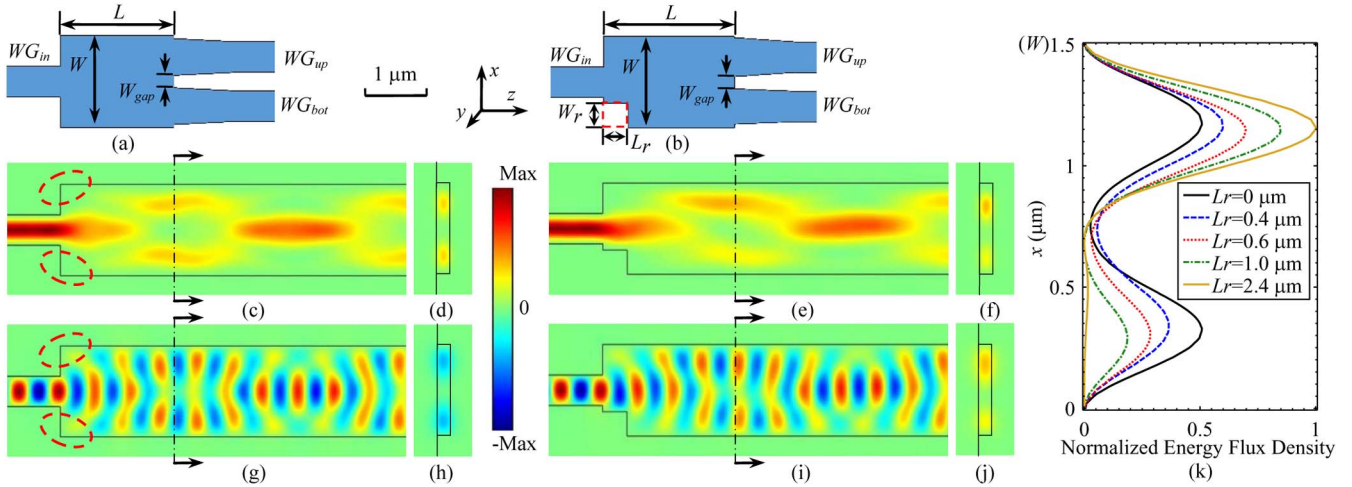


Fig. 1. (a) Schematic, symmetric  $1 \times 2$  MMI power splitter; (b) schematic, asymmetric  $1 \times 2$  MMI power splitter; (c)–(f) optical energy flux density ( $P_z$ ); and (g)–(j) magnetic field ( $H_y$ ) distribution in the multimode region of symmetric [(c), (d), (g), (h)] and asymmetric [(e), (f), (i), (j)] MMI at 1550 nm (wavelength in free space). Cross section view of  $P_z$  [(d), (f)] and  $H_y$  [(h), (j)] distribution at the first two-fold image; (k) normalized energy flux density distribution of the first two-fold image at different removed rectangle length ( $L_r$ ).  $L$  and  $W$ , length and width of the multimode region, respectively;  $W_{\text{gap}}$ , width of the gap between two output waveguides;  $L_r$  and  $W_r$ , length and width of the removed rectangle, respectively. All MMI splitters in this Letter are designed on a SOI platform covered with air, numerically simulated with 3D full vector finite-element method (FEM), and have the following parameter values: thickness of SOI is 220 nm, widths of both input ( $WG_{\text{in}}$ ) and output waveguides ( $WG_{\text{up}}$  and  $WG_{\text{bot}}$ ) are 500 nm,  $W = 1.5 \mu\text{m}$ ,  $W_{\text{gap}} = 200 \text{ nm}$ , and the output waveguides are located at the first two-fold image.

power from  $WG_{\text{up}}$  divided by that from  $WG_{\text{bot}}$ ) quantitatively, the transmitted power from output waveguides is butt-coupled into an optical spectrum analyzer through a tapered lens fiber. The corresponding spectra of an asymmetric MMI power splitter with  $L_r = 0.4 \mu\text{m}$  is shown in Fig. 2(g). Due to the reflection of both end facets, the signal-to-noise ratio is degraded by the Fabry–Perot effect. Trend lines [black solid lines in Fig. 2(g)] are extracted with robust locally weighted regression to suppress noise [21]. To make sure the experimental results are reliable, four identical MMI splitters are fabricated for each group

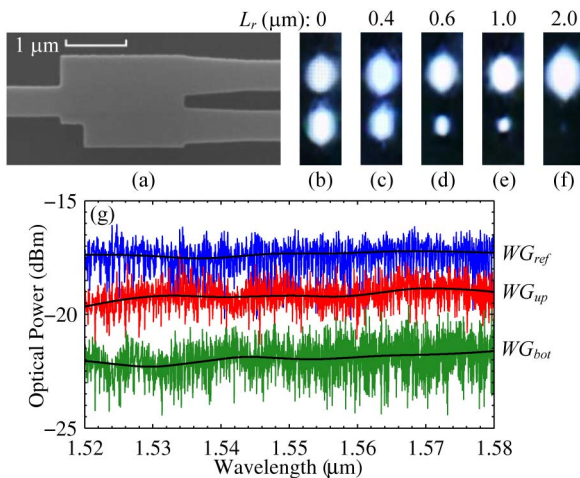


Fig. 2. (a) SEM image of an MMI splitter with  $W_r = 0.4 \mu\text{m}$  and  $L_r = 0.4 \mu\text{m}$ ; (b)–(f) optical images, captured from the output waveguides, of MMI splitters with different removed rectangle length ( $L_r = 0, 0.4, 0.6, 1.0, \text{ and } 2.0 \mu\text{m}$ ); (g) measured spectra of one splitter prototype ( $WG_{\text{up}}$  and  $WG_{\text{bot}}$ );  $WG_{\text{ref}}$ , reference waveguide with the same dimension of  $WG_{\text{up}}$  and  $WG_{\text{bot}}$ ; black solid lines, trend lines extracted with robust locally weighted regression.

of geometric parameters, and the mean values of their measured results are recognized as the final results.

The relations between the PSR and removed rectangle length ( $L_r$ ) are shown in Fig. 3(a), where the measured and simulated results agree quite well. The corresponding multimode region length ( $L$ ) is plotted in Fig. 3(b), which is the actual size for simulations and fabrications. The PSR varies from 50:50 to 100:0 while  $L_r$  increases. At the same time, the first two-fold image shift slightly toward farther position, that is, the length of the multimode region is increasing as shown in the insets of Fig. 3(b). In all cases, the dimension of the multimode region is in the range of  $1.5 \times (1.8\text{--}2.8) \mu\text{m}$ , very compact for large-scale integration.

Further experimental results on wavelength dependence of PSR are shown in Fig. 4. The proportion of optical power output from  $WG_{\text{up}}$  is increasing slightly toward longer working wavelength, which is caused by the intrinsic wavelength dependence of the MMI effect. The variations of PSR are less than 2% for a wavelength range of 60 nm (1520–1580 nm). According to these measurements, we can conclude that the proposed arbitrary-ratio MMI power splitter is weakly dependent on wavelength.

Benefiting from the weak optical energy distribution in the corner, removing the certain region does not introduce any additional loss. The loss property of the proposed splitter is shown in Fig. 5, where the experimental results are normalized with respect to the losses of a single mode stripe waveguide [ $WG_{\text{ref}}$  in Fig. 2(g)]. All the measured losses are higher than the simulations because the loss induced by the roughness of the waveguide sidewalls is not taken into account in simulations. However, both experimental measurements and numerical simulations indicate that the excess loss of arbitrary-ratio MMI power splitter is comparable to a conventional symmetric MMI splitter ( $L_r = 0 \text{ nm}$ ). It is worth

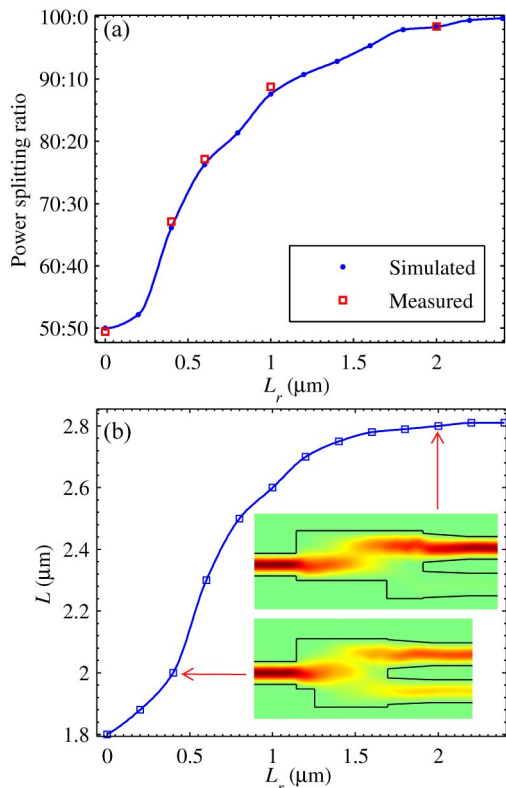


Fig. 3. Relations: (a) PSR at 1550 nm wavelength and (b) corresponding multimode region length ( $L$ ) versus removed rectangle length ( $L_r$ ); the inset shows the optical energy flux density ( $P_z$ ) of an asymmetric MMI splitter with  $L_r = 0.4 \mu\text{m}$  and  $L_r = 2 \mu\text{m}$ .

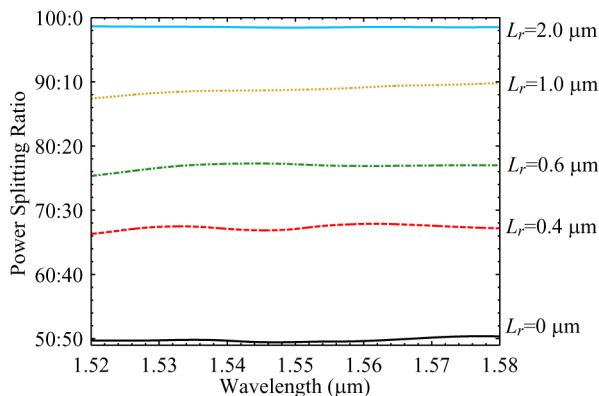


Fig. 4. Wavelength dependence of PSR (measured mean value) at different removed rectangle lengths.

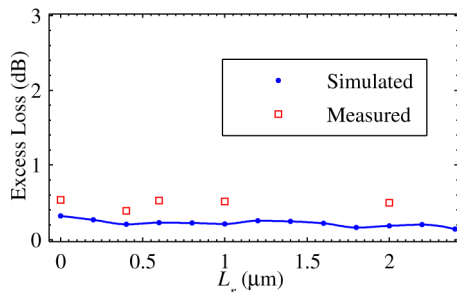


Fig. 5. Excess loss versus removed rectangle length ( $L_r$ ) at 1550 nm wavelength.

mentioning that reducing the gap between the output ports ( $W_{\text{gap}}$ ) will allow more optical power in the multimode region transmitted to the output waveguides, that is, even lower excess loss.

Finally, we numerically analyzed the fabrication tolerance of the removed rectangle, whose length ( $L_r$ ) has been utilized as the control parameter for different PSRs (Fig. 6). The derivative in Fig. 6(a) indicates the maximum variation of PSR is only 0.06% per 1 nm change in  $L_r$ . To analyze the fabrication tolerance further, the removed rectangle width ( $W_r$ ) is changed by  $\Delta W_r$  while the other structural parameters are fixed. The simulations [Fig. 6(b)] show that the PSR variation is less than  $\pm 3\%$ , while the dimension deviates  $\pm 20$  nm from the selected size. All these results demonstrate that the proposed arbitrary-ratio power splitter has a large fabrication tolerance.

In summary, we demonstrated a novel arbitrary-ratio  $1 \times 2$  power splitter based on asymmetric MMI. The device utilizes a very simple structure to achieve an arbitrary power splitting ratio, in which the asymmetry is introduced by removing a certain size corner from the multimode region. Compared to previously reported solutions, the proposed splitters have an extremely compact size of  $1.5 \times (1.8\text{--}2.8) \mu\text{m}$ , while the power splitting ratio can be continuously adjusted from 50:50 to 100:0. Moreover, the measured loss property of the arbitrary-ratio asymmetric MMI power splitters is similar to the conventional symmetric power splitters, which proves that the new structure does not introduce any additional loss. The experimental results also indicate the splitters

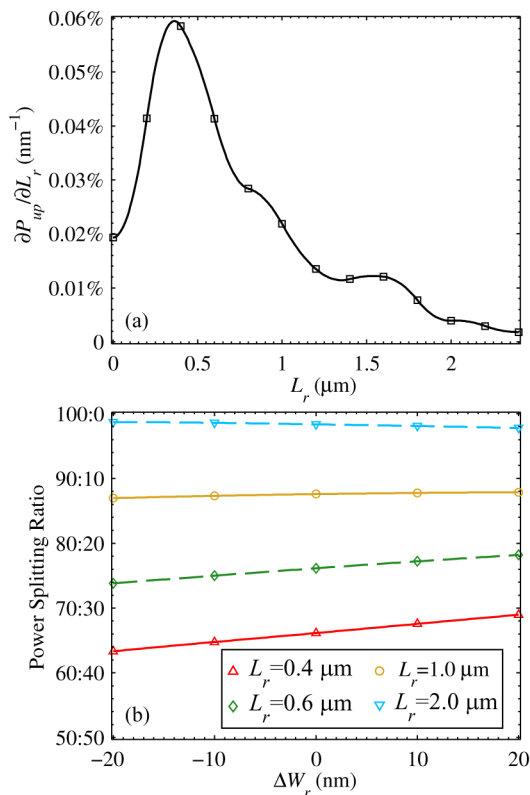


Fig. 6. (a) Derivative of output power from  $\text{WG}_{\text{up}}$  with respect to removed rectangle length ( $L_r$ ) and (b) simulated relations of PSR versus the width variation of removed rectangle ( $\Delta W_r$ ).

are weakly sensitive to wavelength and fabrication imperfections. We demonstrated an arbitrary-ratio  $1 \times 2$  MMI power splitter with a simple and compact structure, while the original advantages of MMI devices are well-kept.

This Letter was partially supported by the Major International Cooperation and Exchange Program of the National Natural Science Foundation of China under Grant 61120106012.

## References

1. L. Thylén and L. Wosinski, *Photon. Res.* **2**, 75 (2014).
2. P. A. Besse, M. Bachmann, H. Melchior, L. B. Soldano, and M. K. Smit, *J. Lightwave Technol.* **12**, 1004 (1994).
3. J. Sun, E. Timurdogan, A. Yaacobi, E. S. Hosseini, and M. R. Watts, *Nature* **493**, 195 (2013).
4. U. Koren, B. I. Miller, M. G. Young, M. Chien, K. Dreyer, R. Ben-Michael, and R. J. Capik, *IEEE Photon. Technol. Lett.* **8**, 364 (1996).
5. M. Mooooka and U. Teruaki, *Opt. Lett.* **34**, 599 (2009).
6. H. Yi, Q. Long, W. Tan, L. Li, X. Wang, and Z. Zhou, *Opt. Express* **20**, 27562 (2012).
7. S. Matsuo, Y. Yoshikuni, T. Segawa, Y. Ohiso, and H. Okamoto, *IEEE Photon. Technol. Lett.* **15**, 1114 (2003).
8. M. Bachmann, P. A. Besse, and H. Melchior, *Appl. Opt.* **34**, 6898 (1995).
9. J. Zhou, H. Shen, R. Jia, H. Liu, Y. Tang, C. Yang, C. Xue, and X. Liu, *Chin. Opt. Lett.* **9**, 82303 (2011).
10. P. A. Besse, E. Gini, M. Bachmann, and H. Melchior, *J. Lightwave Technol.* **14**, 2286 (1996).
11. D. S. D. S. Levy, Y. M. M. Li, R. Scarmozzino, R. M. R. M. Osgood, P. Splitter, D. S. D. S. Levy, Y. M. M. Li, R. Scarmozzino, and R. M. R. M. Osgood, *IEEE Photon. Technol. Lett.* **9**, 1373 (1997).
12. Q. Lai, W. Hunziker, H. Melchior, M. Bachmann, W. Hunziker, P. A. Besse, and H. Melchior, "Arbitrary ratio power splitters using angled silica on silicon multimode interference couplers," in *22nd European Conference on Optical Communication (ECOC)*, Oslo (1996), paper TuC.3.5.
13. S. Tseng, S. Choi, and B. Kippelen, *Opt. Lett.* **34**, 512 (2009).
14. S. Tseng, C. Fuentes-Hernandez, D. Owens, and B. Kippelen, *Opt. Express* **15**, 9015 (2007).
15. D. J. Y. Feng and T. S. Lay, *Opt. Express* **16**, 7175 (2008).
16. D. J. Y. Feng, T. S. Lay, and T. Y. Chang, *Opt. Express* **15**, 1588 (2007).
17. M. Cherchi, S. Ylino, M. Harjanne, M. Kapulainen, T. Vehmas, and T. Aalto, *Opt. Express* **22**, 9245 (2014).
18. T. Saida, A. Himeno, M. Okuno, A. Sugita, K. Okamoto, T. Shimoda, M. Itoh, H. Hatakeyama, T. Tamanuki, and T. Sasaki, *Electron. Lett.* **35**, 2031 (1999).
19. N. S. Lagali, M. R. Paiam, and R. I. MacDonald, *IEEE Photon. Technol. Lett.* **11**, 665 (1999).
20. L. B. Soldano and E. C. M. Pennings, *J. Lightwave Technol.* **13**, 615 (1995).
21. W. S. Cleveland, *J. Am. Stat. Assoc.* **74**, 829 (1979).